UNIVERSAL JOULE HEATING MODEL IN ELECTROPHORETIC SEPARATION MICROCHIPS

Yi Wang, Qiao Lin and Tamal Mukherjee
Carnegie Mellon University, 5000 Forbes Ave., Pittsburgh, PA 15213, USA

Abstract

This paper presents an analytical Joule heating dispersion model for rectangular microchannels. The model holds in all convection-diffusion mass transfer regimes and captures the effects of cross-sectional shape and separation time on JH induced dispersion. The model is verified by three-dimensional numerical simulation and agrees with experimental data from microchip electrophoresis.

Keywords: Joule heating, dispersion, band-broadening, electrophoresis, separations.

1. Introduction

Joule heating (JH) induced analyte dispersion at high electric fields is an important problem in microchip electrophoresis separation, and can play a dominant role in ultra fast electrophoresis [1] and constricted bend designs used for minimizing turn-induced dispersion [2]. Taylor [3] and Aris [4] derived the first model for hydrodynamic dispersion in a circular tube, where diffusion is assumed to be quasi-steady state within the cross section (i.e. Taylor dispersion)[3]. Their results were later adapted to develop a JH dispersion model in circular capillaries [5]. However, microchips typically have non-circular microchannels and can involve transient transverse mass transfer. To address these issues, this paper presents a closed-form JH dispersion model for all mass transfer regimes in rectangular microchannels. Thus, it is generally applicable to practical microchip electrophoresis separation systems.

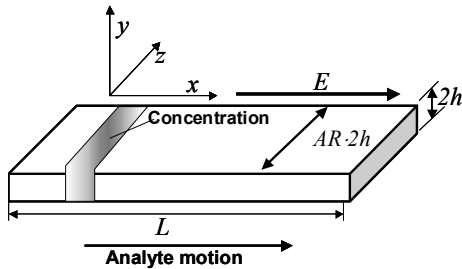## 2. Universal Joule Heating Dispersion Model

Figure 1. Schematic of a micrfabricated electrophoretic separation channel.
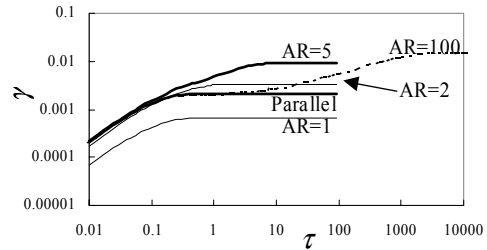

Figure 2. Dependence of γ on time and different aspect ratios.

Consider a microchannel with a rectangular cross section of depth $2h$ and width $AR(2h)$, where AR is the aspect ratio (Fig. 1). An electric field E is applied along the axial direction x, causing the charged analyte to move in a buffer that fills the channel. JH of the buffer due to resistive power $q=k_b \cdot E^2$ where k_b is the buffer's electrical conductivity, causes a non-uniform distribution of the buffer viscosity and temperature, and hence of the analyte velocity u in the cross section. The temperature difference between buffer and channel wall ($\theta=T-T_w$) can be determined as $\theta=\phi \cdot qh^2/k$, where k is the thermal conductivity of buffer, and

ϕ the solution of the canonical heat conduction equation $\nabla^2\phi = -1$ with $\phi = 0$ on the channel walls [6]. Assuming that $\alpha\theta \ll 1$, u can be approximated as $u=u_w(1+\alpha\theta)$, where α is the temperature coefficient of viscosity, and $u_w=\mu_w E$ and μ_w are the analyte velocity and mobility at the wall.

Following the procedure put forward by Aris [4], we can nondimensionalize the governing convective diffusion equation in a coordinate frame that moves at the average analyte velocity U:

$$\begin{cases} \partial c/\partial t = D\cdot\nabla^2 c - u\cdot\partial c/\partial x \\ \partial c/\partial n\big|_\Gamma = 0 \\ c(x,y,z,0)=c_0(x,y,z) \end{cases} \longrightarrow \begin{cases} \partial c/\partial\tau = \partial^2 c/\partial\xi^2 - P_e\cdot\chi\cdot\partial c/\partial x + \overline{\nabla}^2 c \\ \partial c/\partial n\big|_\Gamma = 0 \\ c(\xi,\eta,\zeta,0)=c_0(\xi,\eta,\zeta) \end{cases} \tag{1}$$

where c is the analyte concentration, t separation time, and D the analyte diffusivity. Also, $\xi=(x-Ut)/h$, $\eta=y/h$, $\zeta=z/h$, $\tau=tD/h^2$, $P_e=Uh/D$ (the Peclet number), $\overline{\nabla}^2 = \partial^2/\partial\eta^2 + \partial^2/\partial\zeta^2$ and $\chi=(u-U)/U$ defines the analyte velocity relative to the mean.

Define $m_p(\tau)=\overline{c}_p = \iint_A c_p\,d\eta d\zeta\big/A$ as the pth moment of the cross-section-averaged concentration of the analyte, where $c_p(\eta,\xi,\tau)=\int_{-\infty}^{\infty}\xi^p c(\xi,\eta,\zeta,\tau)d\xi$, A the cross section area of the microchannel. Eq. (1) can be reformulated in terms of m_p and c_p, which can be solved to give the longitudinal variance of the cross-sectional average concentration relative to the moving transverse plane $\xi=0$ by: $\sigma^2=h^2(m_2/m_0-m_1^2/m_0^2)$. The JH dispersivity K, defined as $K=1/2\cdot d(\sigma^2)/dt$, takes the form $K=D+\gamma(\alpha q h^3 u_w/k)^2/D$. The parameter γ captures the effects of channel cross-sectional shape and time on JH dispersion, and is given by

$\gamma = 16\sum_{n=0}^{\infty}\sum_{m=0}^{\infty} S(n)\cdot S(m)\big(1-e^{-4\lambda_{nm}\tau}\big)\cdot\phi_{nm}^2/\lambda_{nm}$. Here, $S(n)=1/2$ for $n=0$ and $S(n)=1$ for $n\geq1$,

$\lambda_{nm}=(n\pi)^2+(m\pi/AR)^2$, $\phi_{00}=0$ and $\phi_{nm} = 4\Big(\int_0^1\int_0^{AR}\phi\cdot\cos(n\pi\eta)\cdot\cos(m\pi\zeta/AR)\cdot d\eta d\zeta\Big)\big/AR$

for $n+m\geq1$. In Fig. 2, we see that γ increases with time and eventually reaches steady state as time becomes sufficiently large. However, for large aspect ratios, γ first reaches a pseudo-steady state around $\tau=0.5$ before approaching the final steady-state value. This corresponds to two distinctly different transverse time constants: $t_1=h^2/D$ for depth-wise diffusion and $t_2=(AR\cdot h)^2/D$ for width-wise diffusion. Fig. 3 shows that the final steady-state values of γ increase with AR until approaching an asymptotic value. It is interesting to note that in both Figs. 2 and 3, the final steady-state value of γ at large AR differs from that for a channel bounded only by parallel plates. This observation is practically significant, as it implies the **inappropriateness** of using a parallel-plate approximation for JH dispersion even at large AR.

3. Numerical simulation and experimental verification

All numerical simulations were performed with CoventorWare. The parameters for the simulations were: $h=15$ μm, $E=6.0$ kV/cm, $t=0.22$ s, $T_w=300$ K, $D=1.0\times10^{-9}$ m^2/s, and $k_b=0.2$ S/m. Figs. 4 and 5 show an excellent match between numerical and analytical results. We also see that the JH dispersivities for AR=1 and parallel plates reach the steady state at the prescribed separation time, while those for AR=2 and AR=5 are still in the transient mass transfer regime, which explains the nonlinear variance increase with time.

Finally, in Fig. 6 our model is compared with the experimental microchip electrophoresis data [1], where Rhodamine B (RB) and Dichlorofluorescein (DCF) were separated. The calculated plate heights for RB and DCF were indistinguishable for practical purposes. Despite limited discrepancies in the plate height $H=\sigma^2/L$ (which may be caused by inaccurate knowledge of geometric and material parameters), the model correctly explains the experimental data. This verifies the validity and usefulness of the model in the design of electrophoresis microchips.
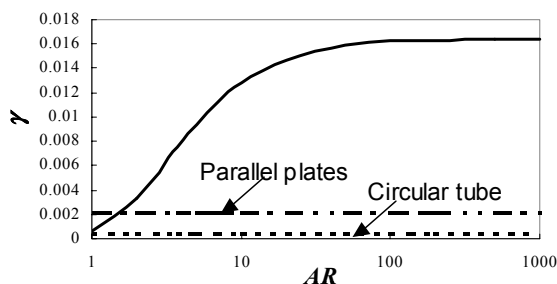
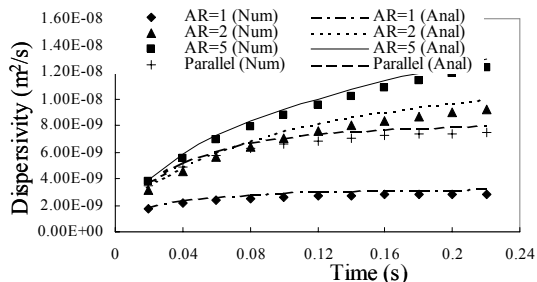Figure 3. Steady state value of γ as a function of the aspect ratio.

Figure 4. Numerical and analytical dispersivity results vs. time for different aspect ratios.
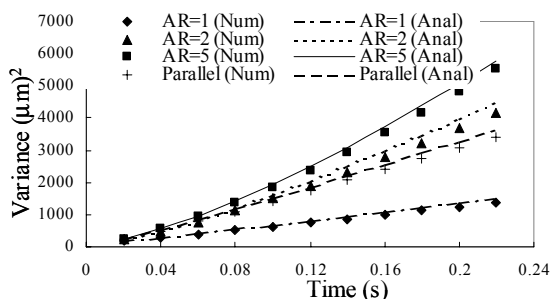

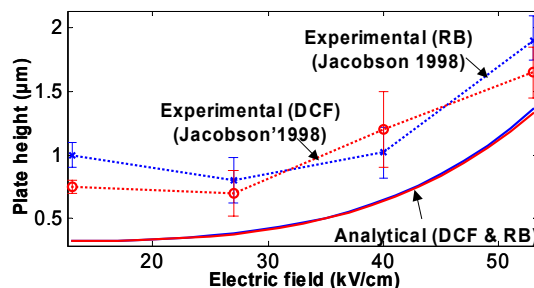Figure 5. Numerical and analytical variance results vs. time for different aspect ratios.

Figure 6. Experimental and analytical plate height results vs. time for different aspect ratios.

4. Conclusion

A universal JH dispersion model has been presented for microchip electrophoresis. The model has been verified by numerical simulation and experimental data, and accurately predicts the effect of cross-sectional shape and separation time on Joule heating dispersion.

References
1. S.C. Jacobson, C.T. Culbertson et al., *Anal. Chem.,* Vol. 70, 3476-3480, 1998.
2. J.I. Molho, A.E. Herr, B.P. Mosier et al., *Anal. Chem.,* Vol. 73, 1350-1360, 2001.
3. G.I. Taylor, *Proc. Roy. Soc. London*, Vol. A219, 186, 1953.
4. R. Aris, *Proc. Roy. Soc. London*, Vol. 235A, 67-77, 1956.
5. J.H. Knox, I.H. Grant, *Chromatographia*, Vol. 24, 135-143, 1987.
6. Y. Wang, Q. Lin, J. Hoburg, T. Mukherjee, *Proc. MSM'02*, 80-83, 2002.